RSC Advances

ROYAL SOCIETY OF CHEMISTRY

www.rsc.org/advances

Structural and Bonding Properties of Small $TiGe_n^-$ (n = 2-6) Clusters: Photoelectron Spectroscopy and Density Functional Calculations

Xiao-Jiao Deng, Xiang-Yu Kong, Xi-Ling Xu, Hong-Guang Xu,* Wei-Jun Zheng*

Beijing National Laboratory for Molecular Sciences, State Key Laboratory of Molecular Reaction Dynamics, Institute of Chemistry, Chinese Academy of Sciences, Beijing 100190, China

***** Corresponding authors. E-mail: xuhong@iccas.ac.cn, zhengwj@iccas.ac.cn

Tel: +86 10 62635054, Fax: +86 10 62563167

Abstract

A number of small $TiGe_n^-$ (n = 2-6) clusters were investigated using anion photoelectron spectroscopy and density functional theory calculations. Their structures were determined by comparison of the theoretical vertical detachment energies and simulated spectra of the low-lying isomers with the experimental results. The most stable structure of $TiGe_n^-$ (n = 2-6) clusters can be considered as a Ti atom substituting one of the Ge atoms in the corresponding Ge_{n+1} cluster or a Ti atom capping a Ge_n cluster (in the case of $TiGe_3^-$). The HOMOs of $TiGe_n^-$ (n = 2-6) clusters are mainly localized on the Ti atom and the Ge atoms interacting directly with the Ti atom.

†**Electronic Supplementary Information (ESI) available**: Cartesian coordinates for stable isomers of $TiGe_n^-$ (n = 2-6) clusters (Table S1). See DOI: 10.1039/c000000x/

1. Introduction

Ti-doped germanium clusters have attracted much attention because they may be used to produce cluster-assembled materials of special electronic and magnetic properties.[1] In addition, it has been suggested that Ti-Ge binary alloys may be developed for dental materials.[2] And it has been found that strain-released hybrid multiplayer Ge-Ti nanomembranes can form anode materials with both high conductivity and high storage capacity, therefore, enhance the performance of lithium batteries.[3] Investigating the structural and electronic properties of Ti-doped germanium clusters may provide valuable information for developing cluster-assembled materials as well as their applications in electronics, biomedicine, and energy storage. In 2002, Kumar and Kawazoe conducted theoretical calculations on a number of transition metal-doped germanium clusters and predicted $TiGe_{16}$ cluster to be a Frank-Kasper polyhedron structure with a large gap between its highest-occupied-molecular-orbital (HOMO) and lowest-unoccupied-molecular-orbital (LUMO).[4] In addition to the $TiGe_{16}$ cluster, the density functional theory (DFT) calculations of Bandyopadhyay et al. on $TiGe_n$ (n = 14-20) suggested that $TiGe_{18}$ cluster also has enhanced stability.[5] And the ground state structure of $TiGe_{12}$ cluster is proposed to be a remarkably stable pseudoicosahedron by Tang et al.[6] More recently, the DFT calculations of $TiGe_n$ (n = 1-20) clusters conducted by Kumar et al. suggested that the Ti atom is encapsulated in the Ge_n cage when n is larger than 9 and the most stable structure of $TiGe_{12}$ cluster is a relaxed hexagon.[7] Compared with the theoretical studies of $TiGe_n$ clusters, the experimental investigation of $TiGe_n$ clusters is quite rare except that Nakajima and co-workers investigated these clusters using mass spectrometry and anion photoelectron spectroscopy, and probed their stability via their reactivity to H_2O adsorption.[8, 9] The HOMO-LUMO gap of neutral $TiGe_{16}$ cluster is estimated to be 1.77 eV based on the photoelectron spectrum of $TiGe_{16}^-$.[8] It is also found that the reactivity of $TiGe_n$ to H_2O decreases dramatically at n = 12.[9]

Nevertheless, the previous anion photoelectron experimental study of $TiGe_n^-$ is limited to cluster size of n = 7-17. In order to get more complete information regarding the bonding properties and structural evolution of $TiGe_n$ clusters, it is very necessary to conduct more detailed studies on the smaller ones. In this work, we report a photoelectron spectroscopy study of $TiGe_n^-$ clusters focusing on small size (n = 2-6) particularly. Also, the geometric structures of these small clusters were determined by comparison of theoretical calculations with photoelectron experiments.

2. Experimental and theoretical methods

2.1 Experiment method

The experiments were conducted on a home-built apparatus equipped with a laser vaporization cluster source, a time-of-flight mass spectrometer, and a magnetic-bottle photoelectron spectrometer, which has been described in elsewhere.[10] The $TiGe_n^-$ (n = 2-6) cluster anions were generated in the laser vaporization source by laser ablation of a rotating translating disk target (13 mm diameter, Ti:Ge mole ratio 1:4) with the second harmonic of a nanosecond Nd:YAG laser (Continuum Surelite II-10). The typical laser power used in this work is about 10 mJ/pulse. Helium gas with ~ 4 atm backing pressure was allowed to expand through a pulsed valve (General Valve Series 9) into the source to cool the formed clusters. The generated cluster anions were mass-analyzed with the time-of-flight mass spectrometer. The cluster anions of interest were selected with a mass gate, decelerated by a momentum decelerator, and crossed with the beam of an Nd:YAG laser (Continuum Surelite II-10, 266 nm) at the photodetachment region. The electrons from photodetachment were energy-analyzed by the magnetic-bottle photoelectron spectrometer. The photoelectron spectra were calibrated with the spectra of Cu^- and Pb^- taken at similar conditions. The resolution of the magnetic-bottle photoelectron spectrometer was about 40 meV at electron kinetic energy of 1 eV.

2.2 Theoretical method

Geometry optimizations of $TiGe_n^-$ (n = 2-6) clusters were performed using density function theory with the Becke's three-parameter and Lee–Yang–Parr's gradient-corrected correlation hybrid functional (B3LYP) [11-13] and 6-311+G(d) basis sets as implemented in the Gaussian 03 program package.[14] The hybrid Heyd-Scuseria-Ernzerhof (HSE06) functional[15-18] was also used to optimize the structure of $TiGe_n^-$ (n = 2-6) clusters. For all clusters, a large amount of initial structures were taken into accounts at all possible spin states. These initial structures were constructed by Ti-capping or Ti-substituting of pure Ge_n clusters or based on the structures of transition metal (TM)-doped Ge_n clusters reported in the literature. All geometries were optimized without any symmetry constraint. Harmonic vibrational frequencies were calculated to make sure that the structures correspond to real local minima, and the zero-point vibrational energy corrections were included for the relative energies of

isomers. The natural population analysis (NPA) of $TiGe_n^-$ clusters was conducted with the Nature Bond Orbital (NBO) version 3.1 program[19-26] implemented in the Gaussian 03 package.

3. Experiment results

The photoelectron spectra of $TiGe_n^-$ (n = 2-6) clusters taken with 266 nm (4.661 eV) photons are shown in Fig. 1, and the vertical detachment energies (VDEs) and adiabatic detachment energies (ADEs) of these clusters estimated from photoelectron spectra are listed in Table 1. The VDEs were estimated from the maxima of the first peaks. The ADEs were determined by drawing a straight line along the leading edge of the first peaks to cross the baseline of spectra and adding the instrument resolution to the electron binding energy (EBE) values at the crossing points.

The spectrum of $TiGe_2^-$ displays three small peaks centered at 1.06, 1.44, and 2.05 eV, as well as a relatively large one at 2.49 eV. As for $TiGe_3^-$, there are six peaks centered at 1.67, 1.95, 2.38, 2.68, 3.20 and 3.43 eV, respectively. The spectrum of $TiGe_4^-$ has two parts, the first one is composed of three resolved peaks centered at 2.17, 2.45 and 2.94 eV, respectively, and the second one has two peaks centered at 3.64 and 3.90 eV. $TiGe_5^-$ has three features centered at 2.87, 3.20 and 3.60 eV, and a large peak above 4.2 eV. There are four major peaks centered at 2.82, 3.20, 3.57 and 4.15 eV in the spectrum of $TiGe_6^-$.

4. Theoretical results

The typical low-lying isomers of $TiGe_n^-$ (n = 2-6) clusters obtained from DFT calculations with B3LYP and HSE06 are similar, the relative energies of these isomers, as well as their theoretical VDEs and ADEs are summarized in Table 2. The theoretical results of both are good agreement with experimental results. Here, we mainly discuss the results of B3LYP in the text. The results of B3LYP are presented in Fig. 2 with the most stable ones on the left. The Cartesian coordinates of the low-lying isomers of $TiGe_n^-$ (n = 2-6) are available in the supplementary material. In addition, we have also simulated the photoelectron spectra of different isomers based on theoretically generalized Koopman theorem,[27, 28] in which each transition corresponds to removal of an electron from a specific molecular orbital of the cluster anion. In the simulation, the first peak associated with the HOMO was set at the

position of theoretical VDE, and the other peaks associated with the deeper orbitals were shifted to higher binding energy side according to the relative energies of the orbitals (ΔE_n). The values of ΔE_n were calculated by equation: $\Delta E_n = E_{HOMO} - E_{HOMO-n}$, where E_{HOMO} is the energy of the HOMO orbital and E_{HOMO-n} is the energy of HOMO-n orbital from theoretical calculations. The peak associated with each orbital was fitted with unit-area Gaussian function of 0.15 eV Full Width at Half Maximum(FWHM). For convenient, we call the simulated spectra as density of states (DOS) spectra. A comparison between the experimental photoelectron spectra and simulated DOS spectra is presented in Fig. 3.

$TiGe_2^-$

The most stable isomer of $TiGe_2^-$ (2A) is a triangle with C_{2v} symmetry. The length of the Ti-Ge bonds is about 2.45 Å and that of the Ge-Ge bond is about 2.53 Å. Its theoretical VDE (1.10 eV) is in good agreement with the experimental value (1.06 eV). The second isomer of $TiGe_2^-$ (2B) has a linear structure with Ti atom locating at one end. It is higher than isomer 2A by 1.09 eV in energy and its theoretical VDE (1.68 eV) is much higher than the experimental value, indicating that its existence in the experiments can be ruled out. As it can be seen in Fig. 3, the simulated DOS spectrum of isomer 2A is in good agreement with experimental spectrum of $TiGe_2^-$. Therefore, isomer 2A is the most probable one detected in our experiments.

$TiGe_3^-$

The most stable isomer of $TiGe_3^-$ (3A) is a tetrahedron with the Ti atom capping the Ge_3 triangle. The next stable isomer (3B) is a rhombus structure with C_{2v} symmetry, which can be seen as Ti atom replacing one Ge atom of Ge_4^- cluster. It is 0.37 eV higher than isomer 3A in energy, and its theoretical VDE (2.10 eV) is much higher than the experimental value (1.67 eV). The theoretical VDE (1.59 eV) of isomer 3A is very close to the experimental value. The simulated DOS spectrum of 3A fits experimental spectrum very well. Isomer 3B is much less stable than 3A. Thus, we suggest isomer 3A to be the most likely structure observed in our experiments.

$TiGe_4^-$

As for $TiGe_4^-$, both isomers 4A and 4B are triangular bipyramid with the Ti atom at different locations. Isomer 4A can also be considered as a Ti atom interacting with a bending Ge_4 rhombus while isomer 4B can be viewed as a Ti atom capping a Ge_4 tetrahedron. Isomer

4B is higher than isomer 4A by only 0.10 eV in energy. Isomer 4C is a quasi-planar structure with two Ge atoms interacting with different edges of $TiGe_2^-$ triangle. The theoretical VDE (1.95 eV) of isomer 4A is in reasonable agreement with the experimental measurement (2.17 eV) and its simulated DOS spectrum resembles the experimental spectrum of $TiGe_4^-$. The theoretical VDE (2.10 eV) of isomer 4B is also close to the experimental value, however, its DOS spectrum is different from the experimental spectrum. We suggest that isomer 4A is the dominant in our experiments, but the existence of 4B cannot be ruled out because it is only slightly less stable than isomer 4A and may contribute to some of the broad photoelectron peaks of $TiGe_4^-$.

$TiGe_5^-$

With respect to $TiGe_5^-$, the most stable isomer (5A) is a C_{4v} symmetry tetragonal bipyramid with the Ti atom at the vertex. Isomer 5B can be viewed as a Ge atom capping the $TiGe_4$ triangular bipyramid. The structure of isomer 5C can be described as the Ti atom connecting to one edge of Ge_4 triangular bipyramid. Isomers 5B and 5C are higher than isomer 5A by 0.63 and 0.95 eV in energy, respectively. The theoretical VDE of 5A (2.90 eV) agrees well with the experimental value (2.87 eV), while those of 5B (2.02 eV) and 5C (1.95 eV) are much lower than experimental value. The simulated DOS spectrum of 5A is also consistent with the experimental spectrum of $TiGe_5^-$. Therefore, we suggest isomer 5A to be the most probable one observed in the experiments.

$TiGe_6^-$

The most stable structure of $TiGe_6^-$ (6A) is a pentagonal bipyramid with the Ti atom at the vertex. Isomer 6B can be described as the Ti atom locating on the top of Ge_6 chair-shaped structure. Isomer 6C can be obtained by having a Ge atom capping one of the upper faces of $TiGe_5$ square bipyramid (5A). The energies of isomers 6B and 6C are much higher than isomer 6A by 0.68 and 0.81 eV, respectively. The calculated VDE (2.98 eV) of 6A is in agreement with the experimental value (2.82 eV), while those of 6B (2.43 eV) and 6C (2.57 eV) deviate from the experimental value. The simulated DOS spectrum of isomer 6A is also in good agreement with the experimental spectrum of $TiGe_6^-$. Therefore, we suggest isomer 6A to be the most probable isomer detected in the experiments.

5. Discussion

In addition to the structures of $TiGe_n^-$ (n = 2-6) clusters, we have also calculated the structures of their corresponding neutrals (Fig. 4). It is found that the most stable structures of $TiGe_n$ (n = 2-5) are similar to those of the anions. The electron affinities (EAs) of neutral clusters can be considered as equal to the ADEs of their corresponding anions when the structures of neutral clusters are very close to those of the anions. Therefore, we estimated the EAs of $TiGe_n$ (n = 2-5) to be 0.78±0.08, 1.43±0.08, 1.97±0.08, and 2.43±0.08 eV respectively based on the ADEs of their anions. The most stable structure of $TiGe_6$ neutral (6A′) can be viewed as a Ge-capped $TiGe_5$ tetragonal bipyramid, which is different from the most stable structure of $TiGe_6^-$ anion (6A). The pentagonal bipyramid style structure (6B′) of $TiGe_6$ neutral is less stable than isomer 6A′ by 0.12 eV. The structures of $TiGe_n$ (n = 2-6) clusters obtained in this work are in agreement with the theoretical calculations of Kumar et al.[7]

Here, we compare the structures of $TiGe_n^-$ clusters with those of pure germanium clusters. The theoretical calculations of $Ge_n^{0,-}$ (n = 1-6) were conducted by Xu et al.[29] and those of $Ge_n^{+,-}$ (n = 5-10) by Li et al.[30] The studies show that the structure of Ge_3 is a triangle, that of Ge_4 a rhombus, Ge_5 a trigonal bipyramid, Ge_6 a tetragonal bipyramid, and Ge_7 a pentagonal bipyramid. From Fig. 2, we can see that the most stable structure of small $TiGe_n^-$ (n = 2-6) clusters can be considered as a Ti atom substituting one of the Ge atoms in the corresponding Ge_{n+1} clusters except that the structure of $TiGe_3^-$ is a tetrahedron, different from the rhombus structure of Ge_4 cluster. Our calculations show that the Ti-Ge bond lengths are in the range of 2.41-2.85 Å and the Ge-Ge bond lengths are in the range of 2.52-2.79 Å in these $TiGe_n^-$ clusters, indicating that the difference between the Ti-Ge and Ge-Ge bond lengths is not significant. That probably is why the substitution of a Ge atom by a Ti atom induced no major change in the structure.

We conduct NPA to investigate the charge on the Ti and Ge atoms and presented them in Table 3. As shown in Table 3, the negative charge on the Ti atom is lower than the sum of negative charge on the Ge atoms because Ge element is more electronegative than Ti. It is different from that of WGe_n cluster reported by Wang et al., in which the W atom possess more negative charge.[31] And it is also different from $TiSi_n^-$ clusters studied by Guo et al., in which charges transfer from Si atoms to Ti atom.[32] That indicates that the charge distributions depend on both the host element and the doped metals. The effective electron configuration on Ti for $TiGe_n^-$ (n = 2-6) clusters are $3d^{2.97}4s^{0.82}4p^{0.31}$, $3d^{3.43}4s^{0.64}4p^{0.31}$, $3d^{3.13}4s^{0.51}4p^{0.45}$, $3d^{3.14}4s^{0.62}4p^{0.54}$ and $3d^{3.05}4s^{0.53}4p^{0.57}$ respectively, indicating that there is hybridization among

the 3*d*, 4*s*, and 4*p* orbitals of Ti atom. To further understand the bonding properties of the $TiGe_n^-$ (n = 2-6) clusters, we plotted the molecular orbital diagrams of the most stable isomers in Fig. 5. It can be seen that the highly occupied molecular orbitals are mainly localized around the Ti atom and the Ge atoms connecting directly with the Ti atom. The localization of the molecular orbitals in Fig. 5 is consistent with the NPA charge distributions of $TiGe_n^-$ clusters in Table 3. It is shown in Table 2 that the lowest-energy isomers for the $TiGe_n^-$ clusters are all in doublet states, indicating that the Ti atom and Ge atom contribute all of their unpaired electrons to form chemical bonds except the excess electron of the negative ions. Besides, from the most stable structures of $TiGe_n^-$ and their neutral, it can be seen that the Ti atom is inclined to interact with more Ge atoms, which is different from the case of Ag atom interacting with Si_n clusters.[33] That probably is due to the existence of unfilled *d* orbitals in Ti atom, which is also in good agreement with the results of NPA charge distributions and molecular orbital analysis.

6. Conclusions

The geometrical structures and growth patterns of small $TiGe_n^-$ (n = 2-6) clusters were investigated by combination of anion photoelectron spectroscopy and DFT calculations. The results show that the most stable structures of these small $TiGe_n^-$ clusters can be considered as a Ti atom substituting one of the Ge atoms in the corresponding Ge_{n+1} cluster or a Ti atom capping a Ge_n cluster. Owing to the existence of multiple unfilled 3*d* orbitals, the Ti atom is inclined to interact with more Ge atoms. The HOMOs of these $TiGe_n^-$ clusters are mainly on the Ti atom and the Ge atoms interacting directly with the Ti atom.

Acknowledgements

W.-J. Z. acknowledges the Knowledge Innovation Program of the Chinese Academy of Sciences (Grant No. KJCX2-EW-H01) and H.-G. X. acknowledges the National Natural Science Foundation of China (Grant No. 21103202) for financial support. The theoretical calculations were conducted on the ScGrid and DeepComp 7000 of the Supercomputing Center, Computer Network Information Center of the Chinese Academy of Sciences.

References

1. X. R. Li, Y. D. Ma, Y. Dai and B. B. Huang, *J. Mater. Chem. C*, 2013, **1**, 4565-4569.
2. W. J. Lin, B. L. Wang, K. J. Qiu, F. Y. Zhou, L. Li, J. P. Lin, Y. B. Wang and Y. F. Zheng, *J. Biomed. Mater. Res. B*, 2012, **100B**, 2239-2250.
3. C. L. Yan, W. Xi, W. P. Si, J. W. Deng and O. G. Schmidt, *Adv. Mater.*, 2013, **25**, 539-544.
4. V. Kumar and Y. Kawazoe, *Phys. Rev. Lett.*, 2002, **88**, 235504.
5. D. Bandyopadhyay, P. Kaur and P. Sen, *J. Phys. Chem. A*, 2010, **114**, 12986-12991.
6. C. M. Tang, M. Y. Liu, W. H. Zhu and K. M. Deng, *Comput. Theor. Chem.*, 2011, **969**, 56-60.
7. M. Kumar, N. Bhattacharyya and D. Bandyopadhyay, *J. Mol. Model.*, 2012, **18**, 405-418.
8. S. Furuse, K. Koyasu, J. Atobe and A. Nakajima, *J. Chem. Phys.*, 2008, **129**, 064311.
9. J. Atobe, K. Koyasu, S. Furuse and A. Nakajima, *Phys. Chem. Chem. Phys.*, 2012, **14**, 9403-9410.
10. H. G. Xu, Z. G. Zhang, Y. Feng, J. Y. Yuan, Y. C. Zhao and W. J. Zheng, *Chem. Phys. Lett.*, 2010, **487**, 204-208.
11. C. T. Lee, W. T. Yang and R. G. Parr, *Phys. Rev. B*, 1988, **37**, 785-789.
12. A. J. H. Wachters, *J. Chem. Phys.*, 1970, **52**, 1033.
13. A. D. Becke, *J. Chem. Phys.*, 1993, **98**, 5648-5652.
14. M. J. Frisch, G. W. Trucks, H. B. Schlegel, et al., *Gaussian, Inc., Wallingford CT, 2004*.
15. J. Heyd, G. E. Scuseria and M. Ernzerhof, *J. Chem. Phys.*, 2003, **118**, 8207-8215.
16. J. Heyd, G. E. Scuseria and M. Ernzerhof, *J. Chem. Phys.*, 2006, **124**, 219906.
17. A. F. Izmaylov, G. E. Scuseria and M. J. Frisch, *J. Chem. Phys.*, 2006, **125**, 104103.
18. A. V. Krukau, O. A. Vydrov, A. F. Izmaylov and G. E. Scuseria, *J. Chem. Phys.*, 2006, **125**, 224106.
19. J. P. Foster and F. Weinhold, *J. Am. Chem. Soc.*, 1980, **102**, 7211-7218.
20. A. E. Reed and F. Weinhold, *J. Chem. Phys.*, 1983, **78**, 4066-4073.
21. A. E. Reed, R. B. Weinstock and F. Weinhold, *J. Chem. Phys.*, 1985, **83**, 735-746.
22. A. E. Reed and F. Weinhold, *J. Chem. Phys.*, 1985, **83**, 1736-1740.
23. J. E. Carpenter and F. Weinhold, *J. Mol. Struct.-THEOCHEM*, 1988, **169**, 41-62.
24. A. E. Reed, L. A. Curtiss and F. Weinhold, *Chem. Rev.*, 1988, **88**, 899-926.
25. J. E. Carpenter, Ph. D. thesis, University of Wisconsin, 1987.
26. F. Weinhold and J. E. Carpenter, in *The Structure of Small Molecules and Ions*, eds. R. Naaman and Z. Vager, 1988, pp. 227-236.
27. D. J. Tozer and N. C. Handy, *J. Chem. Phys.*, 1998, **109**, 10180-10189.
28. J. Akola, M. Manninen, H. Hakkinen, U. Landman, X. Li and L. S. Wang, *Phys. Rev. B*, 1999, **60**, 11297-11300.
29. W. G. Xu, Y. Zhao, Q. S. Li, Y. M. Xie and H. F. Schaefer, *Mol. Phys.*, 2004, **102**, 579-598.
30. B. X. Li, P. L. Cao, B. Song and Z. Z. Ye, *Phys. Lett. A*, 2003, **307**, 318-325.
31. J. Wang and J. G. Han, *J. Phys. Chem. A*, 2006, **110**, 12670-12677.
32. L. J. Guo, X. Liu, G. F. Zhao and Y. H. Luo, *J. Chem. Phys.*, 2007, **126**.
33. X. Y. Kong, X. J. Deng, H. G. Xu, Z. Yang, X. L. Xu and W. J. Zheng, *J. Chem. Phys.*, 2013, **138**, 244312.

Figure Captions:

Fig. 1. Photoelectron spectra of $TiGe_n^-$ (n = 2-6) clusters recorded with 266 nm photons.

Fig. 2. Optimized geometries of the low-lying isomers of $TiGe_n^-$ (n = 2-6) clusters. The relative energies to the most stable isomers (on the left) are shown.

Fig. 3. Comparison between the experimental photoelectron spectra and simulated DOS spectra of the low-lying isomers of $TiGe_n^-$ (n = 2-6) clusters. The simulations were conducted by fitting the distribution of the transition lines with unit-area Gaussian functions of 0.15 eV FWHM.

Fig. 4. Optimized geometries of the low-lying isomers of $TiGe_n$ (n = 2-6) clusters. The relative energies to the most stable isomers (on the left) are shown.

Fig. 5. Molecular orbitals of the most stable isomers of $TiGe_n^-$ (n = 2-6) clusters.

Table 1 Experimental VDEs and ADEs of $TiGe_n^-$ (n = 2-6) clusters obtained from their photoelectron spectra.

cluster	VDE (eV)	ADE (eV)
$TiGe_2^-$	1.06±0.08	0.78±0.08
$TiGe_3^-$	1.67±0.08	1.43±0.08
$TiGe_4^-$	2.17±0.08	1.97±0.08
$TiGe_5^-$	2.87±0.08	2.43±0.08
$TiGe_6^-$	2.82±0.08	2.60±0.08

Table 2 Relative energies of the low-lying isomers of the $TiGe_n^-$ (n = 2-6) obtained by DFT calculations as well as their VDEs and ADEs. The isomers labeled with bold are the probable ones detected in the experiments.

isomer		Sym.	State	ΔE (eV)		VDE (eV)			ADE (eV)		
				B3LYP	HSE06	B3LYP	HSE06	Expt.	B3LYP	HSE06	Expt.
$TiGe_2^-$	**2A**	C_{2v}	$^2A_2$	0	0	1.10	1.07	1.06	1.00	0.98	0.78
	2B	$C_{\infty v}$	^2A	1.09	1.37	1.68	1.19		1.67	0.48	
$TiGe_3^-$	**3A**	C_s	^2A	0	0	1.59	1.57	1.67	1.50	1.47	1.43
	3B	C_{2v}	$^2A_2$	0.37	0.45	2.10	2.02		1.88	1.74	
$TiGe_4^-$	**4A**	C_{2v}	^2A	0	0	1.95	2.12	2.17	1.92	1.94	1.97
	4B	C_s	$^2A"$	0.10	0.13	2.10	2.12		1.81	1.81	
	4C	C_s	^4A	0.51	0.78	2.41	2.35		2.00	2.33	
$TiGe_5^-$	**5A**	C_{4v}	$^2B_2$	0	0	2.90	2.65	2.87	2.77	2.32	2.43
	5B	C_s	^2A	0.63	0.58	2.02	2.14		1.97	2.04	
	5C	C_s	^2A	0.95	0.98	1.95	1.53		1.41	1.33	
$TiGe_6^-$	**6A**	C_1	^2A	0	0	2.98	3.06	2.82	2.79	2.86	2.60
	6B	C_s	^2A	0.68	0.92	2.43	2.62		2.29	2.37	
	6C	C_s	^2A	0.81	0.96	2.57	2.39		2.39	2.19	

Table 3 NPA charge distributions in the most stable isomers of $TiGe_n^-$ (n = 2-6) clusters.

cluster	atom	NPA charge (e)	cluster	atom	NPA charge (e)
$TiGe_2^-$	Ti	-0.10	$TiGe_5^-$	Ti	-0.36
	Ge_1	-0.45		Ge_1	-0.28
	Ge_2	-0.45		Ge_2	-0.09
$TiGe_3^-$	Ti	-0.40		Ge_3	-0.09
	Ge_1	-0.20		Ge_4	-0.09
	Ge_2	-0.20		Ge_5	-0.09
	Ge_3	-0.20	$TiGe_6^-$	Ti	-0.27
$TiGe_4^-$	Ti	-0.14		Ge_1	-0.14
	Ge_1	-0.10		Ge_2	-0.09
	Ge_2	-0.10		Ge_3	-0.14
	Ge_3	-0.33		Ge_4	-0.12
	Ge_4	-0.33		Ge_5	-0.07
				Ge_6	-0.17

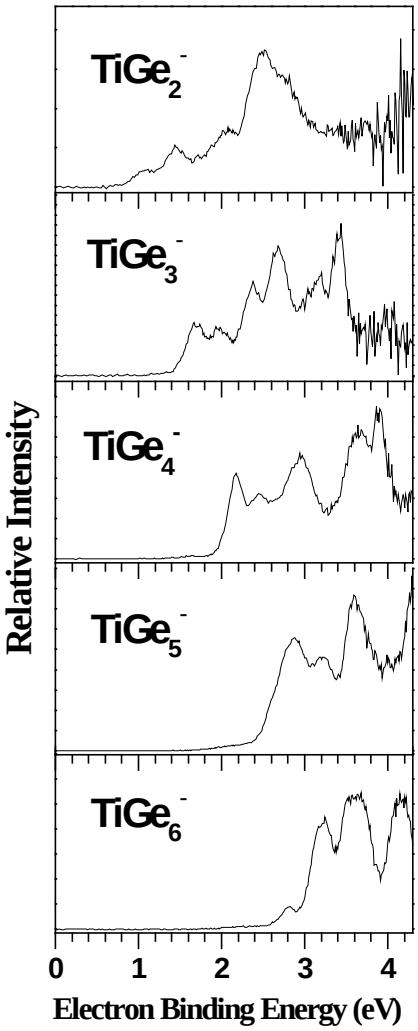

Fig. 1. Photoelectron spectra of $TiGe_n^-$ (n = 2-6) clusters recorded with 266 nm photons.

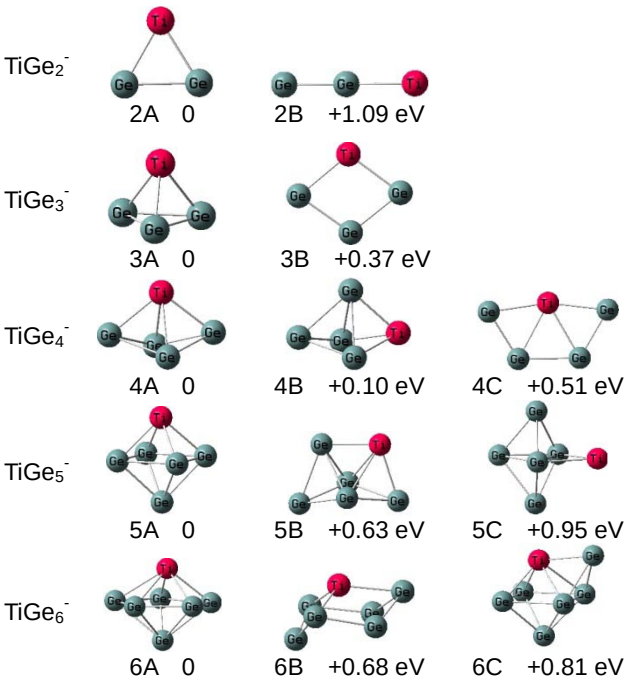

Fig. 2. Optimized geometries of the low-lying isomers of $TiGe_n^-$ (n = 2-6) clusters. The relative energies to the most stable isomers (on the left) are shown.

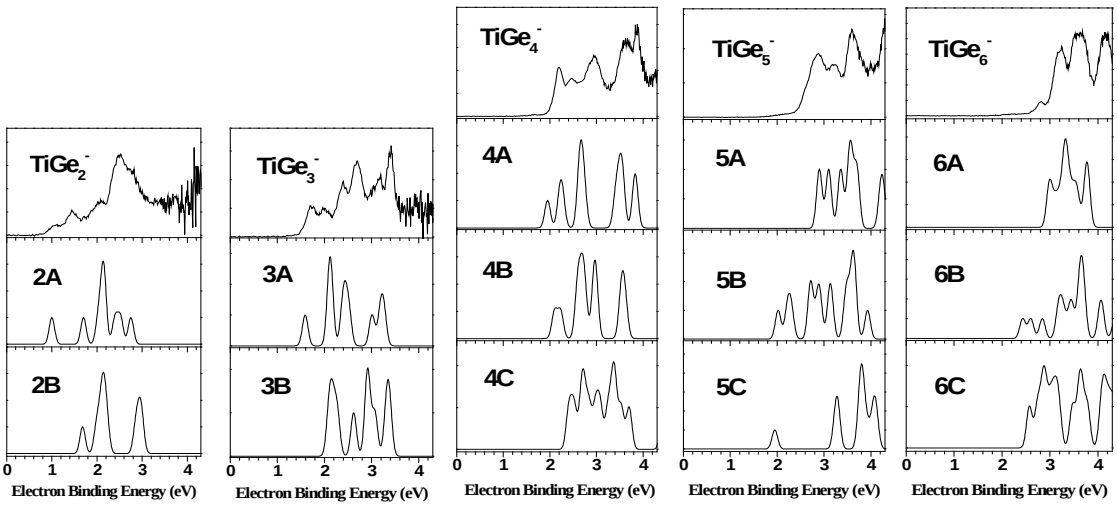

Fig. 3. Comparison between the experimental photoelectron spectra and simulated DOS spectra of the low-lying isomers of $TiGe_n^-$ (n = 2-6) clusters. The simulations were conducted by fitting the distribution of the transition lines with unit-area Gaussian functions of 0.15 eV FWHM.

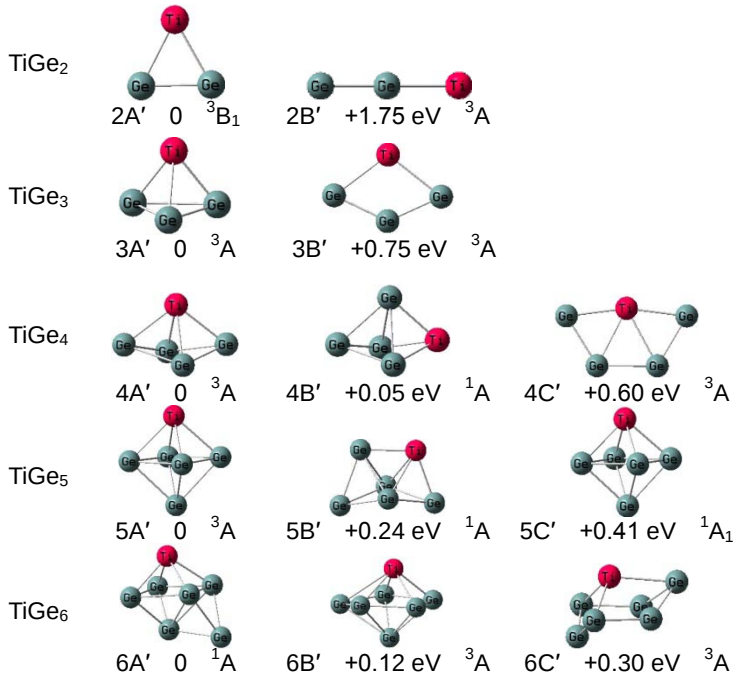

Fig. 4. Optimized geometries of the low-lying isomers of $TiGe_n$ (n = 2-6) clusters. The relative energies to the most stable isomers (on the left) are shown.

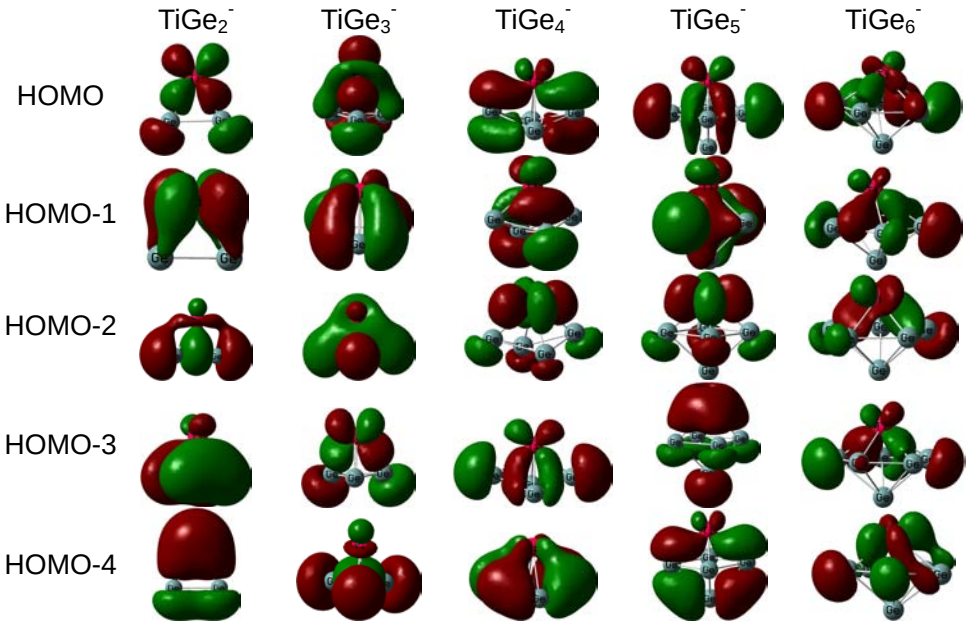

Fig. 5. Molecular orbitals of the most stable isomers of $TiGe_n^-$ (n = 2-6) clusters.

Table of content graphic

The structures of small $TiGe_n^-$ clusters can be considered as Ti-substituted Ge_{n+1} or Ti-capped Ge_n clusters.